HHS Public Access

Author manuscript

J Med Chem. Author manuscript; available in PMC 2024 July 27.

Published in final edited form as:

J Med Chem. 2023 July 27; 66(14): 10027–10035. doi:10.1021/acs.jmedchem.3c00949.

Evaluating Alkaline Phosphatase-Instructed Self-Assembly of D-Peptides for Selectively Inhibiting Ovarian Cancer Cells

Meihui Yi[†], **Zhaoqianqi Feng**[†], **Hongjian He**[†], **Daniela Dinulescu**[‡], **Bing Xu**[*,†]

[†]Department of Chemistry, Brandeis University, 415 South Street, Waltham, MA 02453, USA.

[‡]Department of Pathology, Brigham and Women's Hospital, Harvard Medical School, Boston, MA 02115, USA.

Abstract

Cancer is a major public health concern requiring novel treatment approaches. Enzyme-instructed self-assembly (EISA) provides a unique technique for selectively inhibiting cancer cells. However, structure and activity correlation of EISA remains to be explored. This study investigates new EISA substrates of alkaline phosphatase (ALP) to hinder ovarian cancer cells. Analogues **2–8** were synthesized by modifying the amino acid residues of a potent EISA substrate **1** that effectively inhibits the growth of OVSAHO, a high-grade serous ovarian cancer (HGSOC) cell line. The efficacy of **2–8** against OVSAHO was assessed, along with the combination of substrate **1** with clinically used drugs. The results reveal that substrate **1** displays the highest cytotoxicity against OVSAHO cells, with an IC_{50} of around 8 μM. However, there was limited synergism observed between substrate **1** and the tested clinically used drugs. These findings indicate that EISA likely operates through a distinct mechanism that necessitates further elucidation

Graphical Abstract

[*]**Corresponding Author: Bing Xu** – Department of Chemistry, Brandeis University, 415 South Street, Waltham, MA 02453, USA, bxu@brandeis.edu.

Meihui Yi – Department of Chemistry, Brandeis University, 415 South Street, Waltham, MA 02453, USA

Zhaoqianqi Feng– Department of Chemistry, Brandeis University, 415 South Street, Waltham, MA 02453, USA

Hongjian He – Department of Chemistry, Brandeis University, 415 South Street, Waltham, MA 02453, USA

Daniela Dinulescu – Department of Pathology, Brigham and Women's Hospital, Harvard Medical School, Boston, MA 02115, USA.

Author Contributions

The manuscript was written through contributions of all authors. All authors have given approval to the final version of the manuscript.

Supporting Information.

Supporting information include LC–MS traces and MS of all compounds, experimental details (PDF), and Molecular formula strings and some data (CSV). This material is available free of charge via the Internet at http://pubs.acs.org.

The authors declare no competing financial interest.

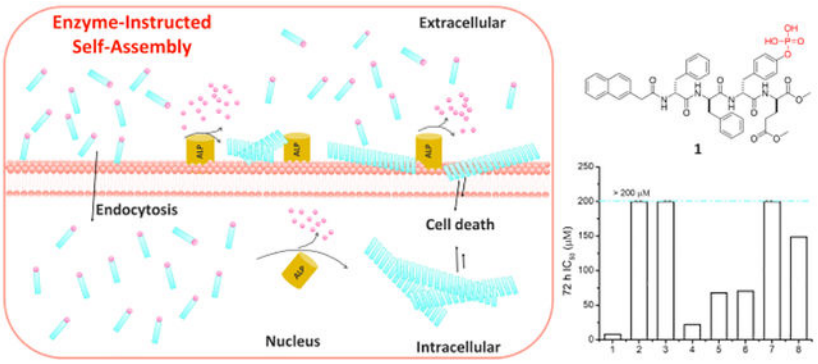

INTRODUCTION

Due to the multiple underlying cellular mechanisms that complicate cancer treatment,[1] cancer remains a major burden to public health.[2] Molecular therapy, mostly based on ligand-receptor interactions, is a key strategy for developing cancer drugs.[3–5] But multiple inherent cellular mechanisms (e.g., up-regulating growth factors or efflux transporters, mutating the drug targets, and increasing metabolic drug degradation[6–10]) work against the drugs that function via ligand-receptor bindings.[11–12] Checkpoint blockade cancer immunotherapy, a recent breakthrough in tumor immune biology,[13–14] can induce long lasting responses in patients with metastatic cancers.[15–21] However, immunosuppression renders immunotherapy ineffective to majority of cancer patients. One of cause of immunosuppression is alkaline phosphatase (ALP), especially in patients with tumor metastasis to bone.[22–24] In tumor microenvironment, ALP rapidly converts adenosine triphosphate (ATP) to adenosine,[25] a major cause for the patients' unresponsiveness to immunotherapy.[26] Thus, ALP is emerging as an important drug target. Although ALP is being recognized as an important target for improving cancer immunotherapy, it is regarded as "undruggable"[27] because it is critical for normal functions of many organs, such as liver and brain.[27–28]

Instead of inhibiting ALP, we have used ALP to catalyze enzyme-instructed self-assembly (EISA) for generating in-situ formed nanofibers to selectively inhibit cancer cells.[29–34] This approach is particularly attractive for targeting high-grade serous ovarian cancer (HGSOC), which also associates with the overexpression of ALP.[35] HGSOC, an aggressive disease with a poor prognosis, is typically diagnosed late in its natural history when tumors have numerous genetic alterations and easily acquire drug resistance.[36–37] This remains a major obstacle in the treatment of ovarian cancers.[38–41] According to the latest report, an estimated 19,710 new cases of ovarian cancer will be diagnosed in the US and 13,270 women will die from the disease in 2023. The majority of death will be caused by HGSOC, as it is the most common and aggressive subtype.[42–49]

To inhibit HGSOC cancer cells that overexpress ALP,[29] such as OVSAHO, we have been developing EISA substrates. In our previous study, we have identified a D-peptide[50] as the EISA substrate that effectively inhibits OVSAHO without harming hepatocytes. Although that work[29, 51] established a molecular design to target HGSOCs that overexpress ALP, several questions remain to be answered. For example, what is the structure-activity

relationships of that molecular architecture and whether the EISA substrates would be suitable to combine with other clinically used drugs for inhibit HGSOCs.

To answer the above questions, we designed and synthesized seven analogs of a potent phosphopeptide-based EISA substrate (**1**) by adding hydrophobic amino acid residue in the peptide backbone (**2**-**6**) or mitochondria targeting motif at the side chain of the phosphopeptides (**7**-**8**). The precursors largely contain D-peptides as the backbones because D-peptides are proteolytic resistant and D-tyrosine phosphate can be dephosphorylated by enzymes such as alkaline phosphatase[50]. Our results show that the IC_{50} values of **2**, **3** and **7** are greater than 200 μM, the IC_{50} values of **4** is smaller than 12.5 μM, and the IC_{50} values of **5**, **6** and **8** are 46.9 μM, 70.5 μM and 148.7 μM, respectively.

We also used the combination of **1** with clinically used drugs (Doxorubicin, Cisplatin, Paclitaxel, BAY 11–7085, K252A, LOC14, PACMA31, Talazoparib, and Bortezomib) and tested them against one of the most resistant HGSOC cell line, OVSAHO. However, our results show that clinical drugs and **1** exhibit limited synergy. These results support that EISA operates on fundamentally new mechanisms for inhibiting OVSAHO and underscore the importance of further elucidating the mechanism of action of EISA.

RESULTS AND DISCUSSION

Molecular design.

As shown in Scheme 2, we designed the EISA precursor **1**, which contains a naphthyl capping group (Nap) at the N-terminal, D-diphenylalanine (ff) in the middle backbone, D-phosphotyrosine (y_p) as an ALP cleavage site, and D-glutamic acid dimethyl ester at the C-terminal. Based on the structure of **1**, by adding one more D-phenylalanine, D-leucine, or L-leucine before or after the ff backbone, we obtained precursor **2**-**6** to study the influence of molecular structure on biological activity. Keeping the structure of Nap-ffy_p, we added a D-lysine at the C-terminal and connected triphenyl phosphonium (TPP), a mitochondria-targeting motif, to the side chain of lysine to produce **7**. By changing Nap to NBD-β-alanine, we obtained precursor **8**. We expect that **7** and **8** would target mitochondria of cancer cells, and **8** would be a useful molecule to reveal the cellular location of the assemblies of the dephosphorylated **8** after ALP removes the phosphate group from **8** and triggers self-assembly. As shown in the critical aggregation concentrations (CAC) of the precursors (Figure S3), the addition of more hydrophobic amino acids, such as phenylalanine and leucine, to the backbone of **1** increases the self-assembly ability of the precursors (2–6). However, when TPP cation is attached to the side chain of **1**, the resulting precursors (**7** and **8**) are more hydrophilic and less prone to self-assembling.

Synthesis.

We first used solid phase peptide synthesis (SPPS) to synthesize all peptides without methylation or connecting the TPP to the side chain of lysine (Scheme S1). Briefly, the fluorenylmethyloxycarbonyl (Fmoc)-protected amino acid was attached to the 2-chlorotrityl chloride resin. After the addition of 20% piperidine in N, N dimethylformamide (DMF) to release the Fmoc group, the next amino acid or capping group was attached to expand the

chain of the peptide or cap the peptide chain. Then, trifluoroacetic acid was added to cleave the products from the resin. To obtain methylated substrates **1–6**, the obtained peptides (1 equivalent) were dissolved in dichloromethane with stirring and then bromotrimethylsaline (30 equivalent) was added. The reaction was stirred at room temperature overnight. After air drying, methanol was added, and the reaction was stirred at room temperature for 1 day. After purification by HPLC, substrates **1–6** were obtained. For the production of substrates **7** and **8**, TPP was first activated by 1.1 equivalent N-hydroxysuccinimide (NHS) and N, N'-dicyclohexylcarbodiimide (DCC) with catalytic amount of 4-dimethylamiopryidine in dichloromethane. After obtaining the activated TPP filtrate by filtration and evaporated, it was dissolved in DMF, and the corresponding peptides (1.3 equivalent) was added with 3 equivalent N-diisopropylethylamine (DIEA). The reaction mixture was stirred overnight, and the products were purified with HPLC.

Inhibitory activity.

After obtaining the pure EISA substrates, we firstly tested the cell viability of different ovarian cancer cell lines incubated with substrate **1**. Substrate **1** exhibits the most potent cytotoxicity against OVSAHO and OVSAHO-luc cell lines with the 72 h IC_{50} of 8.0 μM and 9.8 μM, respectively. This indicates that OVSAHO transfected with luciferase showed similar behavior to the OVSAHO cell line. In addition to these two cell lines, Kuramochi is also sensitive to **1**, with a 72 h IC_{50} around 18.2 μM. However, **1** is less potent against GEMM4412 and JHOS4 cell lines, with IC_{50} values of 172.9 μM and 194.7 μM, respectively. Further, **1** exhibits much less cytotoxicity toward CHOK, SKOV3, OVCAR3, OVCAR4, OVCAR5, GEMM4306, A2780-res, and A2780 cells, with 72 h IC_{50} values greater than 200 μM (Figure 1A). The low potency of **1** against these cells agrees with that none of them overexpresses ALP.[52]

To further examine the cytotoxicity of other precursors and based on the previous cell viability data, we chose OVSAHO cells as the cell line for testing the cytotoxicity of the analogs of **1**. According to the 72 h IC_{50} of all precursors (Figure 1B), the potency of all the precursors follows the order of **1**> **4**> **5**, 6> **8**> **2**, **3**, **7**. Apparently, the insertion of D-leucine between ff and D-pTyr largely maintains the potency of the EISA precursor. However, the insertion of D-leucine before the diphenylalanine greatly decreases the activity of the precursor. The insertion of the hydrophobic L-leucine before and after the diphenylalanine shows the efficacy of inhibiting OVSAHO, but it is less potent compared to precursor **1**. The introduction of TPP dramatically decreases the activity of the precursors, suggesting that OVSAHO is less dependent on mitochondria for survival. Although adding a phenylalanine increases the self-assembling ability of the peptides, the activity drops even more. The structure variations of **1** indicates that the attachment of TPP cation at the side chain of **1** or the insertion of extra hydrophobic D-amino acid residue group at the N-terminal of **1** significantly decreases the activity of **1**. However, the insertion of a hydrophobic L-amino acid residue at the N-terminal of **1** only slightly decreases the activity of the precursor. These results indicate that the supramolecular structures of the assemblies likely determine the activity of EISA and further structural change is necessary for developing precursors more potent than **1**.

Combination with drugs.

Combination of multiple anticancer drugs is a commonly used strategy to enhance cancer therapy efficiency in chemotherapy.[53–54] Based on the high efficiency of substrate **1** compared to other derivatives and the potency of precursor **1** against OVSAHO cell compared to other cell lines, we chose substrate **1** and OVSAHO cell to further test the combination of **1** with drugs used in clinic. As shown in the three-days cell viability data (Figure 3), the IC_{50} of **1** is greater than, approximate, and below 20 μM in day 1, 2, and 3, respectively. The significant increase of the inhibition efficiency from 24 to 72 h is likely a result of the accumulation of the assemblies of **1** inside the cancer cells. This observation is consistent with that EISA precursors inhibit cancer cells without acquired drug resistance[55]. Since 20 μM of **1** is quite biocompatible to OVSAHO on the first day and the efficacy of the combination of substrate **1** with clinical drug is important in day 1, we chose **1** at 20 μM for the combination study. We selected nine commercial drugs based on their different functions in inhibiting cancer cells, including doxorubicin, cisplatin, paclitaxel, BAY11–7085, K252A, LOC14, PACMA31, talazoparib, and bortezomib (BTZ). As shown in Figure 2, when OVSAHO cells were treated with **1** combined with doxorubicin for 24 h, the cell viability greatly dropped from about 120% to 20%. Combining **1** with cisplatin, BAY11–7085, and K252A slightly enhances inhibiting OVSAHO cells. No inhibition enhancement occurred when OVSAHO cells were cocultured with substrate **1** and paclitaxel, LOC14, PACMA31, talzaoparib, or BTZ.

The 24 h cytotoxicity of doxorubicin itself against OVSAHO is around 75% at concentration of 1.25 μM, 2.5 μM, and 5 μM (Figure 3D). However, the cell viability hardly decreases further with the dosage increase of doxorubicin (Figure 2). To explore the enhanced efficacy of OVSAHO cell inhibition observed in the coculture of **1** and doxorubicin, we conducted further investigation involving combinations of concentrations and treatment times. When the concentration of substrate **1** is below 5 μM, the cytotoxicity is primarily attributed to doxorubicin, as the cell viability of combinational group is similar to that of doxorubicin treated group. Notably, significant enhancements are observed when the concentrations of precursor **1** are 1o μM or 20 μM (Figure 3A). Similar results are observed for all three-day combinations (Figure 3B, C).

CONCLUSION

In summary, we have designed a series of peptide substrates of ALP to examine the structure-activity relationship based on **1**. The introduction of one additional hydrophobic amino acid, such as leucine or phenylalanine, in the backbones does not significantly increase the potency of the substrates. The lower activities of **2**-**6** likely originate from the less rigid nanofibers that those of formed after dephosphorylation, as suggested by transmission electron microscopy of the self-assembled nanostructures (Figure S1, 2). Although it is know that the position of phosphates can affect the activity of the EISA precursors[56], in this work, the position of phosphates in the precursors is less likely to affect the activity because the positions of the phosphates are the same (from the C-terminal). In addition, further combination of designed precursor with clinical drugs suggests that designed precursor exerts a unique way of cancer cell killing. These results suggest that

the exploration of structural variations[57–58] beyond amino acid addition to the peptide backbone, and further elucidation the detailed mechanism of **1** for inhibiting OVSAHO is necessary.

EXPERIMENTAL SECTION

General Information.

2-Chlorotrityl chloride resin (1.0–1.2mmol/g), O-(benzotriazol-1-yl)-N, N, N', N'-tetramethyluronium hexafluorophosphate (HBTU), and Fmoc-protected amino acids were purchased from GL Biochem (Shanghai, China). Bromotrimethylsilane was purchased from Sigma-Aldrich. Other chemical reagents and solvents were purchased from Fisher Scientific. All chemical reagents and solvents were used as received from commercial sources without further purification. All ovarian cancer cell lines were provided by Doctor Daniela M. Dinulescu. RPMI1640 medium was purchased from American Type Culture Collection (ATCC, USA). McCoy's 5A Medium, Dulbecco's modified Eagle medium, fetal bovine serum, and Gibco penicillin–streptomycin were purchased from Life Technologies. All precursors were purified with an Agilent 1100 Series Liquid Chromatograph system, equipped with an XTerra C18 RP column and a Variable Wavelength Detector. The LC–MS spectra were obtained with a Waters Acquity Ultra Performance LC with Waters MICROMASS detector.

Synthesis of Desired Compounds.

We synthesized all peptides without methylation using SPPS. Weighing 0.5 g (0.5 equivalent) of 2-chlorotrityl chloride resin, we immersed it in methylene chloride (DCM) for 15 min. The Fmoc protected amino acids were weighed according to 1.2 mmol/g of resin. We dissolved the Fmoc protected amino acid in DCM, adding 2.5 equivalent of N, N-Diisopropylethylamine (DIEA). Then, we thoroughly mixed the resin with the solution well on a rocker for 1 h. We washed it with DCM, followed by the addition of capping solution (DCM: MeOH: DIEA= 17: 2: 1) and reacted for 15 min. Afterward, we washed it with DCM first and then dimethylformamide (DMF). Using 20% piperidine in DMF for 30 min, we removed the Fmoc group. We washed it with DMF and loaded the next Fmoc protected amino acid (1 equivalent), HBTU (1 equivalent), and DIEA (2.5 equivalent) in DMF for 40 min. We washed it with DMF. Upon finishing the addition of all amino acids, we used DCM to wash out DMF. For peptide cleavage, we employed a mixture of 95% TFA, 2.5% triisopropyl silane (TIPS), 2.5% H2O for 60 min. We removed trifluoroacetic acid with air flow and precipitated the residue with diethyl ether. Finally, we collected the product for further synthesis.

The crude product (1 equivalent) from SPPS was dissolved in DCM with stirring and then bromotrimethylsaline (15 equivalent) was added. The reaction mixture was stirred at room temperature overnight. After air drying, methanol was added, and the reaction was stirred at room temperature for 1 day. Then the product (**1–6**) was purified with HPLC.

To a solution of 100 mg of 3-carboxypropyl triphenylphosphonium bromide (TPP) in 10 mL of dichloromethane (DCM), by 1.1 equiv. (29 mg) of N-Hydroxysuccinimide (NHS)

and 57.6 mg of N, N'-dicyclohexylcarbodiimide (DCC) were added, along with catalytic amount of 4-dimethylamiopyridine. The mixture was stirred at room temperature for 2 h, and then filtered through a filter paper to remove precipitates. The filtrate was evaporated under reduced pressure, resulting in a white power that was used directly for the next step.

The white powder obtained above was dissolved in 5 mL of N, N-dimethylformamide, and then 1.3 equivalents of corresponding peptide were added, along with 3 equiv. N-diisopropylethylamine (DIPEA). The resulting reaction mixture was stirred overnight, and the products (**7–8**) were purified by reverse phase HPLC. The purity of the compounds was determined using LC-MS. (Figure S4–11) All compounds are >95% pure by HPLC analysis.

Supplementary Material

Refer to Web version on PubMed Central for supplementary material.

ACKNOWLEDGMENT

This work is partially supported by NIH CA142746 and CA252364.

ABBREVIATION

ALP	alkaline phosphatase
HGSOC	high-grade serous ovarian cancer
ATP	adenosine triphosphate
EISA	enzyme-instructed self-assembly
BTZ	Bortezomib
TPP	triphenyl phosphonium
Nap	2-Naphthaleneacetic acid
NBD	7-nitrobenzofurazan
SPPS	solid phase peptide synthesis
Fmoc	fluorenylmethyloxycarbonyl
DMF	N, N dimethylformamide
NHS	N-hydroxysuccinimide
DCC	N, N'- dicyclohexylcarbodiimide
DIEA	N-diisopropylethylamine
DCM	methylene chloride
HBTU	O-(benzotriazol-1-yl)-N,N,N',N-tetramethyluronium hexafluorophosphate

TFA	trifluoroacetic acid
TIPS	triisopropyl silane

REFERENCES

1. Hanahan D; Weinberg RA, Hallmarks of cancer: The next generation. Cell 2011, 144 (5), 646–674. [PubMed: 21376230]
2. Siegel RL; Miller KD; Jemal A, Cancer statistics, 2020. CA Cancer J Clin 2020, 70 (1), 7–30. [PubMed: 31912902]
3. Fiskus W; Mitsiades N, B-Raf Inhibition in the Clinic: Present and Future. In Annual Review of Medicine, Vol 67, Caskey CT, Ed. 2016; Vol. 67, pp 29–43.
4. Rimawi MF; Schiff R; Osborne CK, Targeting HER2 for the Treatment of Breast Cancer. In Annual Review of Medicine, Vol 66, Caskey CT, Ed. 2015; Vol. 66, pp 111–128.
5. Lord CJ; Tutt ANJ; Ashworth A, Synthetic Lethality and Cancer Therapy: Lessons Learned from the Development of PARP Inhibitors. In Annual Review of Medicine, Vol 66, Caskey CT, Ed. 2015; Vol. 66, pp 455–470.
6. Samimi G; Safaei R; Katano K; Holzer AK; Rochdi M; Tomioka M; Goodman M; Howell SB, Increased Expression of the Copper Efflux Transporter ATP7A Mediates Resistance to Cisplatin, Carboplatin, and Oxaliplatin in Ovarian Cancer Cells. Clin. Cancer Res 2004, 10 (14), 4661–4669. [PubMed: 15269138]
7. Mozzetti S; Ferlini C; Concolino P; Filippetti F; Raspaglio G; Prislei S; Gallo D; Martinelli E; Ranelletti FO; Ferrandina G; Scambia G, Class III beta-tubulin overexpression is a prominent mechanism of paclitaxel resistance in ovarian cancer patients. Clin. Cancer Res 2005, 11 (1), 298–305. [PubMed: 15671559]
8. Rodland KD; Bollinger N; Ippolito D; Opresko LK; Coffey RJ; Zangar R; Wiley HS, Multiple Mechanisms Are Responsible for Transactivation of the Epidermal Growth Factor Receptor in Mammary Epithelial Cells. J. Biol. Chem 2008, 283 (46), 31477–31487. [PubMed: 18782770]
9. Liu X; Chan D; Ngan H, Mechanisms of chemoresistance in human ovarian cancer at a glance. OB/GYN 2012, 2 (3), 100–104.
10. Pyragius CE; Fuller M; Ricciardelli C; Oehler MK, Aberrant lipid metabolism: an emerging diagnostic and therapeutic target in ovarian cancer. Int. J. Mol. Sci 2013, 14 (4), 7742–56. [PubMed: 23574936]
11. Gottesman MM, Mechanisms of cancer drug resistance. Annu. Rev. Med 2002, 53 (1), 615–627. [PubMed: 11818492]
12. Gottesman MM; Lavi O; Hall MD; Gillet JP, Toward a Better Understanding of the Complexity of Cancer Drug Resistance. In Annual Review of Pharmacology and Toxicology, Vol 56, Insel, P. A., Ed. 2016; Vol. 56, pp 85–102.
13. Krummel MF; Allison JP, CD28 AND CTLA-4 HAVE OPPOSING EFFECTS ON THE RESPONSE OF T-CELLS TO STIMULATION. Journal of Experimental Medicine 1995, 182 (2), 459–465. [PubMed: 7543139]
14. Ishida Y; Agata Y; Shibahara K; Honjo T, INDUCED EXPRESSION OF PD-1, A NOVEL MEMBER OF THE IMMUNOGLOBULIN GENE SUPERFAMILY, UPON PROGRAMMED CELL-DEATH. Embo Journal 1992, 11 (11), 3887–3895. [PubMed: 1396582]
15. Sanmamed MF; Chen L, A Paradigm Shift in Cancer Immunotherapy: From Enhancement to Normalization. Cell 2018, 175 (2), 313–326. [PubMed: 30290139]
16. Hodi FS; O'Day SJ; McDermott DF; Weber RW; Sosman JA; Haanen JB; Gonzalez R; Robert C; Schadendorf D; Hassel JC; Akerley W; van den Eertwegh AJM; Lutzky J; Lorigan P; Vaubel JM; Linette GP; Hogg D; Ottensmeier CH; Lebbe C; Peschel C; Quirt I; Clark JI; Wolchok JD; Weber JS; Tian J; Yellin MJ; Nichol GM; Hoos A; Urba WJ, Improved Survival with Ipilimumab in Patients with Metastatic Melanoma. New England Journal of Medicine 2010, 363 (8), 711–723. [PubMed: 20525992]
17. Robert C; Thomas L; Bondarenko I; O'Day S; Weber J; Garbe C; Lebbe C; Baurain J-F; Testori A; Grob J-J; Davidson N; Richards J; Maio M; Hauschild A; Miller WH Jr.; Gascon

P; Lotem M; Harmankaya K; Ibrahim R; Francis S; Chen T-T; Humphrey R; Hoos A; Wolchok JD, Ipilimumab plus Dacarbazine for Previously Untreated Metastatic Melanoma. New England Journal of Medicine 2011, 364 (26), 2517–2526. [PubMed: 21639810]

18. Wolchok JD; Kluger H; Callahan MK; Postow MA; Rizvi NA; Lesokhin AM; Segal NH; Ariyan CE; Gordon R-A; Reed K; Burke MM; Caldwell A; Kronenberg SA; Agunwamba BU; Zhang X; Lowy I; Inzunza HD; Feely W; Horak CE; Hong Q; Korman AJ; Wigginton JM; Gupta A; Sznol M, Nivolumab plus Ipilimumab in Advanced Melanoma. New England Journal of Medicine 2013, 369 (2), 122–133. [PubMed: 23724867]
19. Maude SL; Frey N; Shaw PA; Aplenc R; Barrett DM; Bunin NJ; Chew A; Gonzalez VE; Zheng Z; Lacey SF; Mahnke YD; Melenhorst JJ; Rheingold SR; Shen A; Teachey DT; Levine BL; June CH; Porter DL; Grupp SA, Chimeric Antigen Receptor T Cells for Sustained Remissions in Leukemia. New England Journal of Medicine 2014, 371 (16), 1507–1517. [PubMed: 25317870]
20. Postow MA; Chesney J; Pavlick AC; Robert C; Grossmann K; McDermott D; Linette GP; Meyer N; Giguere JK; Agarwala SS; Shaheen M; Ernstoff MS; Minor D; Salama AK; Taylor M; Ott PA; Rollin LM; Horak C; Gagnier P; Wolchok JD; Hodi FS, Nivolumab and Ipilimumab versus Ipilimumab in Untreated Melanoma. New England Journal of Medicine 2015, 372 (21), 2006–2017. [PubMed: 25891304]
21. Dong HD; Strome SE; Salomao DR; Tamura H; Hirano F; Flies DB; Roche PC; Lu J; Zhu GF; Tamada K; Lennon VA; Celis E; Chen LP, Tumor-associated B7-H1 promotes T-cell apoptosis: A potential mechanism of immune evasion. Nature Medicine 2002, 8 (8), 793–800.
22. Karhade AV; Thio QCBS; Kuverji M; Ogink PT; Ferrone ML; Schwab JH, Prognostic value of serum alkaline phosphatase in spinal metastatic disease. British Journal of Cancer 2019, 120 (6), 640–646. [PubMed: 30792532]
23. Karhade AV; Thio QCBS; Ogink PT; Shah AA; Bono CM; Oh KS; Saylor PJ; Schoenfeld AJ; Shin JH; Harris MB; Schwab JH, Development of Machine Learning Algorithms for Prediction of 30-Day Mortality After Surgery for Spinal Metastasis. Neurosurgery 2018.
24. Karhade AV; Thio QCBS; Ogink PT; Schwab JH, Serum alkaline phosphatase and 30-day mortality after surgery for spinal metastatic disease. Journal of Neuro-Oncology 2018, 140 (1), 165–171. [PubMed: 30173410]
25. Di Virgilio F; Sarti AC; Falzoni S; De Marchi E; Adinolfi E, Extracellular ATP and P2 purinergic signalling in the tumour microenvironment. Nature Reviews Cancer 2018, 18 (10), 601–618. [PubMed: 30006588]
26. Vijayan D; Young A; Teng MWL; Smyth MJ, Targeting immunosuppressive adenosine in cancer. Nature Reviews Cancer 2017, 17 (12), 709–724. [PubMed: 29059149]
27. Millán JL, Mammalian Alkaline Phosphatases: From Biology to Applications in Mdicine and Biotechnology. John Wiley & Sons: 2006.
28. Fonta C; Négyessy L, Neuronal Tissue-Nonspecific Alkaline Phosphatase (TNAP). Springer, 2015.
29. Feng Z; Wang H; Zhou R; Li J; Xu B, Enzyme-Instructed Assembly and Disassembly Processes for Targeting Downregulation in Cancer Cells. J Am Chem Soc 2017, 139 (11), 3950–3953. [PubMed: 28257192]
30. Feng Z; Han X; Wang H; Tang T; Xu B, Enzyme-Instructed Peptide Assemblies Selectively Inhibit Bone Tumors. Chem 2019, 5 (9), 2442–2449. [PubMed: 31552305]
31. Pires RA; Abul-Haija YM; Costa DS; Novoa-Carballal R; Reis RL; Ulijn RV; Pashkuleva I, Controlling Cancer Cell Fate Using Localized Biocatalytic Self-Assembly of an Aromatic Carbohydrate Amphiphile. Journal of the American Chemical Society 2015, 137 (2), 576–579. [PubMed: 25539667]
32. Gao G; Jiang Y-W; Zhan W; Liu X; Tang R; Sun X; Deng Y; Xu L; Liang G, Trident Molecule with Nanobrush–Nanoparticle–Nanofiber Transition Property Spatially Suppresses Tumor Metastasis. Journal of the American Chemical Society 2022, 144 (26), 11897–11910. [PubMed: 35731698]
33. Ding Y; Zheng D; Xie L; Zhang X; Zhang Z; Wang L; Hu Z-W; Yang Z, Enzyme-Instructed Peptide Assembly Favored by Preorganization for Cancer Cell Membrane Engineering. Journal of the American Chemical Society 2023, 145 (8), 4366–4371. [PubMed: 36669158]

34. Tanaka A; Fukuoka Y; Morimoto Y; Honjo T; Koda D; Goto M; Maruyama T, Cancer Cell Death Induced by the Intracellular Self-Assembly of an Enzyme-Responsive Supramolecular Gelator. Journal of the American Chemical Society 2015, 137 (2), 770–775. [PubMed: 25521540]

35. Luo M; Zhou L; Zhan SJ; Cheng LJ; Li RN; wang H; Liu B; Linghu H, ALPL regulates the aggressive potential of high grade serous ovarian cancer cells via a non-canonical WNT pathway. Biochem. Biophys. Res. Commun 2019, 513 (2), 528–533. [PubMed: 30979497]

36. Yap TA; Carden CP; Kaye SB, Beyond chemotherapy: targeted therapies in ovarian cancer. Nat. Rev. Cancer 2009, 9 (3), 167–181. [PubMed: 19238149]

37. Deretic D; Huber LA; Ransom N; Mancini M; Simons K; Papermaster DS, SMALL G-PROTEIN RAB8 MAY PARTICIPATE IN ROS DISK MORPHOGENESIS IN PHOTORECEPTORS. Investigative Ophthalmology & Visual Science 1994, 35 (4), 2151–2151.

38. Jelovac D; Armstrong DK, Recent Progress in the Diagnosis and Treatment of Ovarian Cancer. CA-Cancer J. Clin 2011, 61 (3), 183–203. [PubMed: 21521830]

39. Galluzzi L; Vitale I; Michels J; Brenner C; Szabadkai G; Harel-Bellan A; Castedo M; Kroemer G, Systems biology of cisplatin resistance: past, present and future. Cell Death & Disease 2014, 5.

40. Cornelison R; Llaneza DC; Landen CN, Emerging Therapeutics to Overcome Chemoresistance in Epithelial Ovarian Cancer: A Mini-Review. International Journal of Molecular Sciences 2017, 18 (10).

41. Binju M; Padilla MA; Singornat T; Kaur P; Rahmanto YS; Cohen PA; Yu Y, Mechanisms underlying acquired platinum resistance in high grade serous ovarian cancer - a mini review. Biochimica Et Biophysica Acta-General Subjects 2019, 1863 (2), 371–378. [PubMed: 30423357]

42. Jonsson J-M; Johansson I; Dominguez-Valentin M; Kimbung S; Jonsson M; Bonde JH; Kannisto P; Masback A; Malander S; Nilbert M; Hedenfalk I, Molecular Subtyping of Serous Ovarian Tumors Reveals Multiple Connections to Intrinsic Breast Cancer Subtypes. Plos One 2014, 9 (9).

43. Bell D; Berchuck A; Birrer M; Chien J; Cramer DW; Dao F; Dhir R; DiSaia P; Gabra H; Glenn P; Godwin AK; Gross J; Hartmann L; Huang M; Huntsman DG; Iacocca M; Imielinski M; Kalloger S; Karlan BY; Levine DA; Mills GB; Morrison C; Mutch D; Olvera N; Orsulic S; Park K; Petrelli N; Rabeno B; Rader JS; Sikic BI; Smith-McCune K; Sood AK; Bowtell D; Penny R; Testa JR; Chang K; Dinh HH; Drummond JA; Fowler G; Gunaratne P; Hawes AC; Kovar CL; Lewis LR; Morgan MB; Newsham IF; Santibanez J; Reid JG; Trevino LR; Wu YQ; Wang M; Muzny DM; Wheeler DA; Gibbs RA; Getz G; Lawrence MS; Cibulskis K; Sivachenko AY; Sougnez C; Voet D; Wilkinson J; Bloom T; Ardlie K; Fennell T; Baldwin J; Gabriel S; Lander ES; Ding L; Fulton RS; Koboldt DC; McLellan MD; Wylie T; Walker J; O'Laughlin M; Dooling DJ; Fulton L; Abbott R; Dees ND; Zhang Q; Kandoth C; Wendl M; Schierding W; Shen D; Harris CC; Schmidt H; Kalicki J; Delehaunty KD; Fronick CC; Demeter R; Cook L; Wallis JW; Lin L; Magrini VJ; Hodges JS; Eldred JM; Smith SM; Pohl CS; Vandin F; Raphael BJ; Weinstock GM; Mardis R; Wilson RK; Meyerson M; Winckler W; Getz G; Verhaak RGW; Carter SL; Mermel CH; Saksena G; Nguyen H; Onofrio RC; Lawrence MS; Hubbard D; Gupta S; Crenshaw A; Ramos AH; Ardlie K; Chin L; Protopopov A; Zhang J; Kim TM; Perna I; Xiao Y; Zhang H; Ren G; Sathiamoorthy N; Park RW; Lee E; Park PJ; Kucherlapati R; Absher DM; Waite L; Sherlock G; Brooks JD; Li JZ; Xu J; Myers RM; Laird PW; Cope L; Herman JG; Shen H; Weisenberger DJ; Noushmehr H; Pan F; Triche T Jr.; Berman BP; Van den Berg DJ; Buckley J; Baylin SB; Spellman PT; Purdom E; Neuvial P; Bengtsson H; Jakkula LR; Durinck S; Han J; Dorton S; Marr H; Choi YG; Wang V; Wang NJ; Ngai J; Conboy JG; Parvin B; Feiler HS; Speed TP; Gray JW; Levine DA; Socci ND; Liang Y; Taylor BS; Schultz N; Borsu L; Lash AE; Brennan C; Viale A; Sander C; Ladanyi M; Hoadley KA; Meng S; Du Y; Shi Y; Li L; Turman YJ; Zang D; Helms EB; Balu S; Zhou X; Wu J; Topal MD; Hayes DN; Perou CM; Getz G; Voet D; Saksena G; Zhang J; Zhang H; Wu CJ; Shukla S; Cibulskis K; Lawrence MS; Sivachenko A; Jing R; Park RW; Liu Y; Park PJ; Noble M; Chin L; Carter H; Kim D; Karchin R; Spellman PT; Purdom E; Neuvial P; Bengtsson H; Durinck S; Han J; Korkola JE; Heiser LM; Cho RJ; Hu Z; Parvin B; Speed TP; Gray JW; Schultz N; Cerami E; Taylor BS; Olshen A; Reva B; Antipin Y; Shen R; Mankoo P; Sheridan R; Ciriello G; Chang WK; Bernanke JA; Borsu L; Levine DA; Ladanyi M; Sander C; Haussler D; Benz CC; Stuart JM; Benz SC; Sanborn JZ; Vaske CJ; Zhu J; Szeto C; Scott GK; Yau C; Hoadley KA; Du Y; Balu S; Hayes DN; Perou CM; Wilkerson MD; Zhang N; Akbani R; Baggerly KA; Yung WK; Mills GB; Weinstein JN; Penny R; Shelton T; Grimm D; Hatfield M; Morris S; Yena P; Rhodes P; Sherman M; Paulauskis J; Millis S; Kahn A; Greene JM; Sfeir R; Jensen MA; Chen J; Whitmore J; Alonso

S; Jordan J; Chu A; Zhang J; Barker A; Compton C; Eley G; Ferguson M; Fielding P; Gerhard DS; Myles R; Schaefer C; Shaw KRM; Vaught J; Vockley JB; Good PJ; Guyer MS; Ozenberger B; Peterson J; Thomson E; Canc Genome Atlas Res, N., Integrated genomic analyses of ovarian carcinoma. Nature 2011, 474 (7353), 609–615. [PubMed: 21720365]

44. Ledermann J; Harter P; Gourley C; Friedlander M; Vergote I; Rustin G; Scott C; Meier W; Shapira-Frommer R; Safra T; Matei D; Macpherson E; Watkins C; Carmichael J; Matulonis U, Olaparib Maintenance Therapy in Platinum-Sensitive Relapsed Ovarian Cancer. New England Journal of Medicine 2012, 366 (15), 1382–1392. [PubMed: 22452356]
45. Domcke S; Sinha R; Levine DA; Sander C; Schultz N, Evaluating cell lines as tumour models by comparison of genomic profiles. Nature Communications 2013, 4.
46. Patch A-M; Christie EL; Etemadmoghadam D; Garsed DW; George J; Fereday S; Nones K; Cowin P; Alsop K; Bailey PJ; Kassahn KS; Newell F; Quinn MCJ; Kazakoff S; Quek K; Wilhelm-Benartzi C; Curry E; Leong HS; Hamilton A; Mileshkin L; Au-Yeung G; Kennedy C; Hung J; Chiew Y-E; Harnett P; Friedlander M; Quinn M; Pyman J; Cordner S; O'Brien P; Leditschke J; Young G; Strachan K; Waring P; Azar W; Mitchell C; Traficante N; Hendley J; Thorne H; Shackleton M; Miller DK; Arnau GM; Tothill RW; Holloway TP; Semple T; Harliwong I; Nourse C; Nourbakhsh E; Manning S; Idrisoglu S; Bruxner TJC; Christ AN; Poudel B; Holmes O; Anderson M; Leonard C; Lonie A; Hall N; Wood S; Taylor DF; Xu Q; Fink JL; Waddell N; Drapkin R; Stronach E; Gabra H; Brown R; Jewell A; Nagaraj SH; Markham E; Wilson PJ; Ellul J; McNally O; Doyle MA; Vedururu R; Stewart C; Lengyel E; Pearson JV; Waddell N; deFazio A; Grimmond SM; Bowtell DDL; Australian Ovarian Canc Study, G., Whole-genome characterization of chemoresistant ovarian cancer. Nature 2015, 521 (7553), 489–494. [PubMed: 26017449]
47. Zhang Q; Wang C; Cliby WA, Cancer-associated stroma significantly contributes to the mesenchymal subtype signature of serous ovarian cancer. Gynecologic Oncology 2019, 152 (2), 368–374. [PubMed: 30448260]
48. McDonald ME; Salinas EA; Devor EJ; Newtson AM; Thiel KW; Goodheart MJ; Bender DP; Smith BJ; Leslie KK; Gonzalez-Bosquet J, Molecular Characterization of Non-responders to Chemotherapy in Serous Ovarian Cancer. International Journal of Molecular Sciences 2019, 20 (5).
49. Bowtell DD; Boehm S; Ahmed AA; Aspuria P-J; Bast RC Jr.; Beral V; Berek JS; Birrer MJ; Blagden S; Bookman MA; Brenton JD; Chiappinelli KB; Martins FC; Coukos G; Drapkin R; Edmondson R; Fotopoulou C; Gabra H; Galon J; Gourley C; Heong V; Huntsman DG; Iwanicki M; Karlan BY; Kaye A; Lengyel E; Levine DA; Lu KH; McNeish IA; Menon U; Narod SA; Nelson BH; Nephew KP; Pharoah P; Powell DJ Jr.; Ramos P; Romero IL; Scott CL; Sood AK; Stronach EA; Balkwill FR, Rethinking ovarian cancer II: reducing mortality from high-grade serous ovarian cancer. Nature Reviews Cancer 2015, 15 (11), 668–679. [PubMed: 26493647]
50. Li J; Gao Y; Kuang Y; Shi J; Du X; Zhou J; Wang H; Yang Z; Xu B, Dephosphorylation of d-Peptide Derivatives to Form Biofunctional, Supramolecular Nanofibers/Hydrogels and Their Potential Applications for Intracellular Imaging and Intratumoral Chemotherapy. Journal of the American Chemical Society 2013, 135 (26), 9907–9914. [PubMed: 23742714]
51. Feng Z; Wang H; Zhou R; Li J; Xu B, Enzyme-Instructed Assembly and Disassembly Processes for Targeting Downregulation in Cancer Cells. Journal of the American Chemical Society 2017, 139 (11), 3950–3953. [PubMed: 28257192]
52. Barretina J; Caponigro G; Stransky N; Venkatesan K; Margolin AA; Kim S; Wilson CJ; Lehar J; Kryukov GV; Sonkin D; Reddy A; Liu M; Murray L; Berger MF; Monahan JE; Morais P; Meltzer J; Korejwa A; Jane-Valbuena J; Mapa FA; Thibault J; Bric-Furlong E; Raman P; Shipway A; Engels IH; Cheng J; Yu GK; Yu J; Aspesi P Jr.; de Silva M; Jagtap K; Jones MD; Wang L; Hatton C; Palescandolo E; Gupta S; Mahan S; Sougnez C; Onofrio RC; Liefeld T; MacConaill L; Winckler W; Reich M; Li N; Mesirov JP; Gabriel SB; Getz G; Ardlie K; Chan V; Myer VE; Weber BL; Porter J; Warmuth M; Finan P; Harris JL; Meyerson M; Golub TR; Morrissey MP; Sellers WR; Schlegel R; Garraway LA, The Cancer Cell Line Encyclopedia enables predictive modelling of anticancer drug sensitivity. Nature 2012, 483 (7391), 603–7. [PubMed: 22460905]
53. Bonadonna G; Zucali R; Monfardini S; de Lena M; Uslenghi C, Combination chemotherapy of Hodgkin's disease with adriamycin, bleomycin, vinblastine, and imidazole carboxamide versus MOPP. Cancer 1975, 36 (1), 252–259. [PubMed: 54209]

54. Dai G; Sun L; Xu J; Zhao G; Tan Z; Wang C; Sun X; Xu K; Zhong W, Catechol–metal coordination-mediated nanocomposite hydrogels for on-demand drug delivery and efficacious combination therapy. Acta Biomaterialia 2021, 129, 84–95. [PubMed: 34010690]

55. Wang H; Feng Z; Wang Y; Zhou R; Yang Z; Xu B, Integrating Enzymatic Self-Assembly and Mitochondria Targeting for Selectively Killing Cancer Cells without Acquired Drug Resistance. Journal of the American Chemical Society 2016, 138 (49), 16046–16055. [PubMed: 27960313]

56. Zhou J; Du X; Yamagata N; Xu B, Enzyme-Instructed Self-Assembly of Small d-Peptides as a Multiple-Step Process for Selectively Killing Cancer Cells. Journal of the American Chemical Society 2016, 138 (11), 3813–3823. [PubMed: 26966844]

57. Bolarinwa O; Nimmagadda A; Su M; Cai J, Structure and Function of AApeptides. Biochemistry 2017, 56 (3), 445–457. [PubMed: 28029249]

58. Wu D; Sinha N; Lee J; Sutherland BP; Halaszynski NI; Tian Y; Caplan J; Zhang HV; Saven JG; Kloxin CJ; Pochan DJ, Polymers with controlled assembly and rigidity made with click-functional peptide bundles. Nature 2019, 574 (7780), 658–662. [PubMed: 31666724]

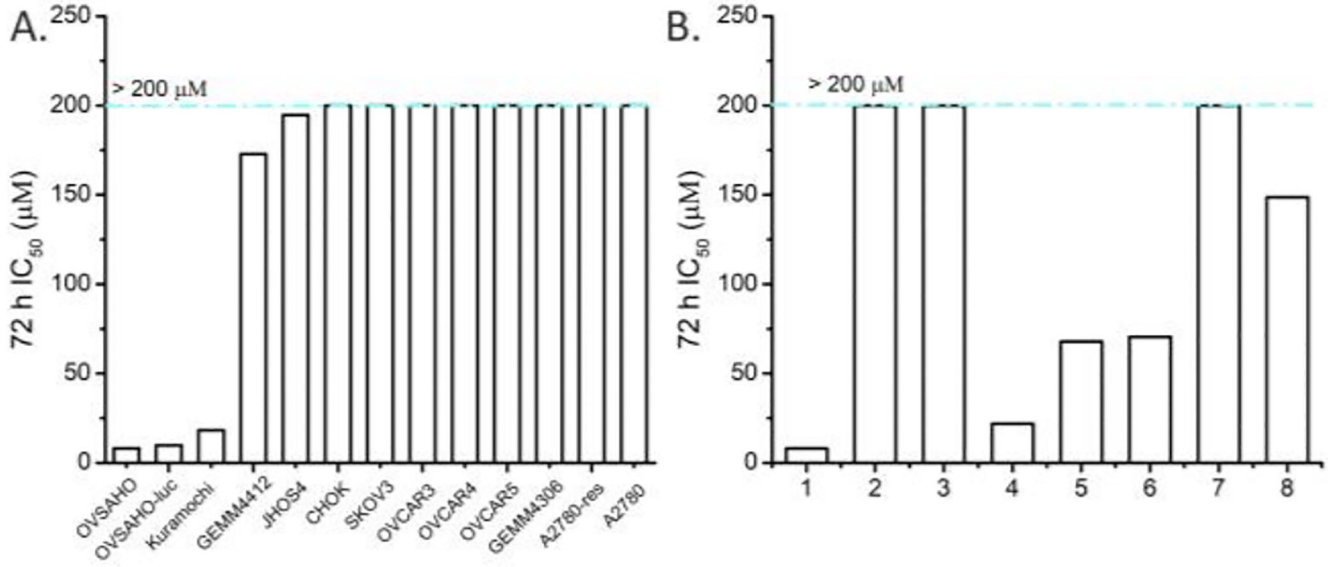

Figure 1.

A. The 72 h IC_{50} of **1** against OVSAHO, OVSAHO-luc, Kuramochi, GEMM 4412, JHOS4, CHOK, SKOV3, OVCAR3, OVCAR4, OVCAR5, GEMM4306, A2780-res, and A2780 cells. B. The 72 h IC_{50} of **1**, **2**, **3**, **4**, **5**, **6**, **7**, and **8** against OVSAHO cells.

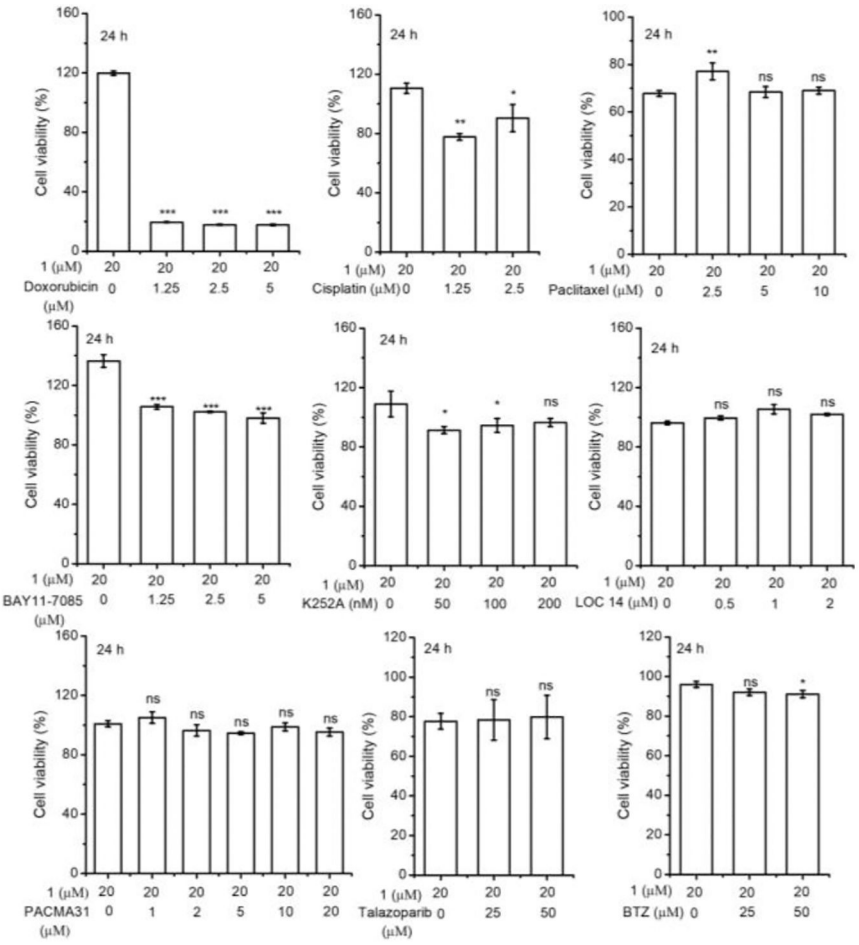

Figure 2.

The cell viability of OVSAHO treated with **1** (20 μM) and the combination of **1** and doxorubicin, cisplatin, paclitaxel, BAY11–7085, K252A, LOC14, PACMA31, talazoparib, and BTZ for 24 h. $p > 0.05$ (ns), $p < 0.05$ (*), $p < 0.01$ (**), $p < 0.001$ (***).

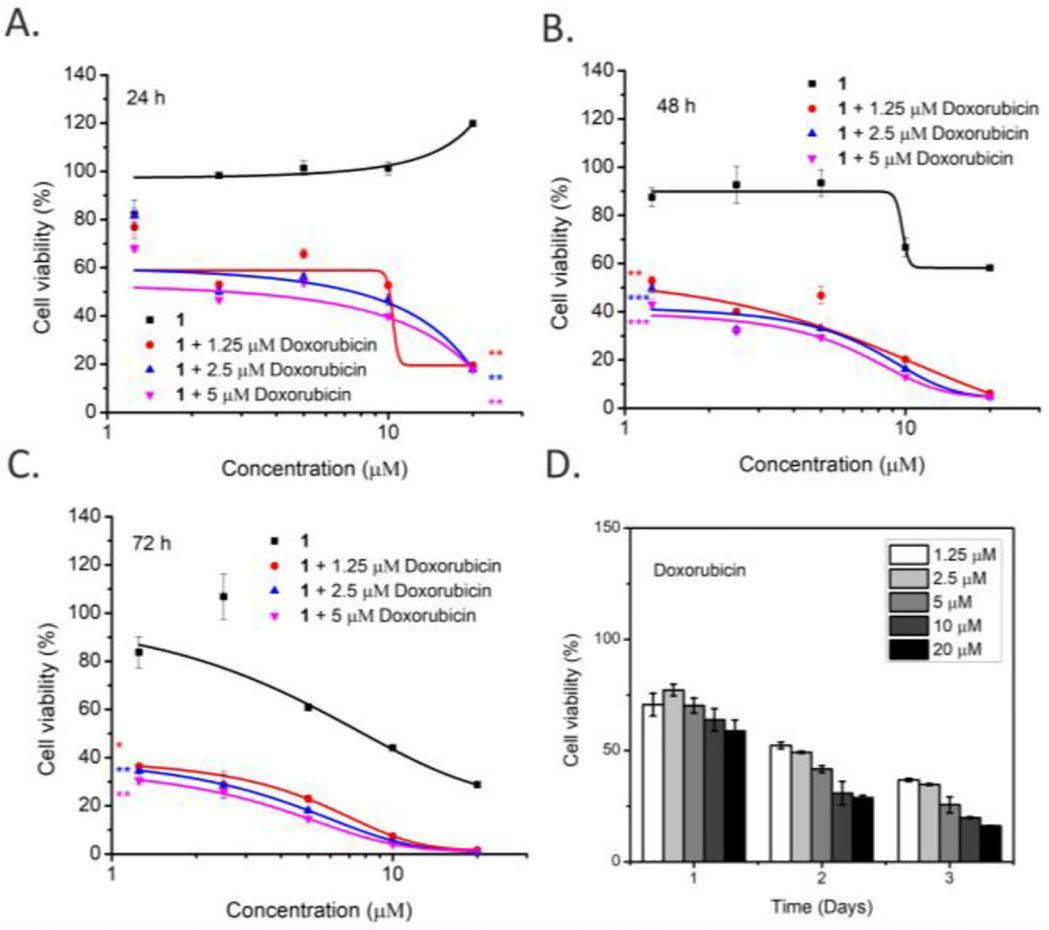

Figure 3.

The cell viability of OVSAHO treated with **1**, doxorubicin and the combination of **1** and doxorubicin for A) 24 h, B) 48 h, and C) 72 h. D. The cell viability of OVSAHO treated with doxorubicin for 24 h, 36 h, and 72 h. $p > 0.05$ (ns), $p < 0.05$ (*), $p < 0.01$ (**), $p < 0.001$ (***).

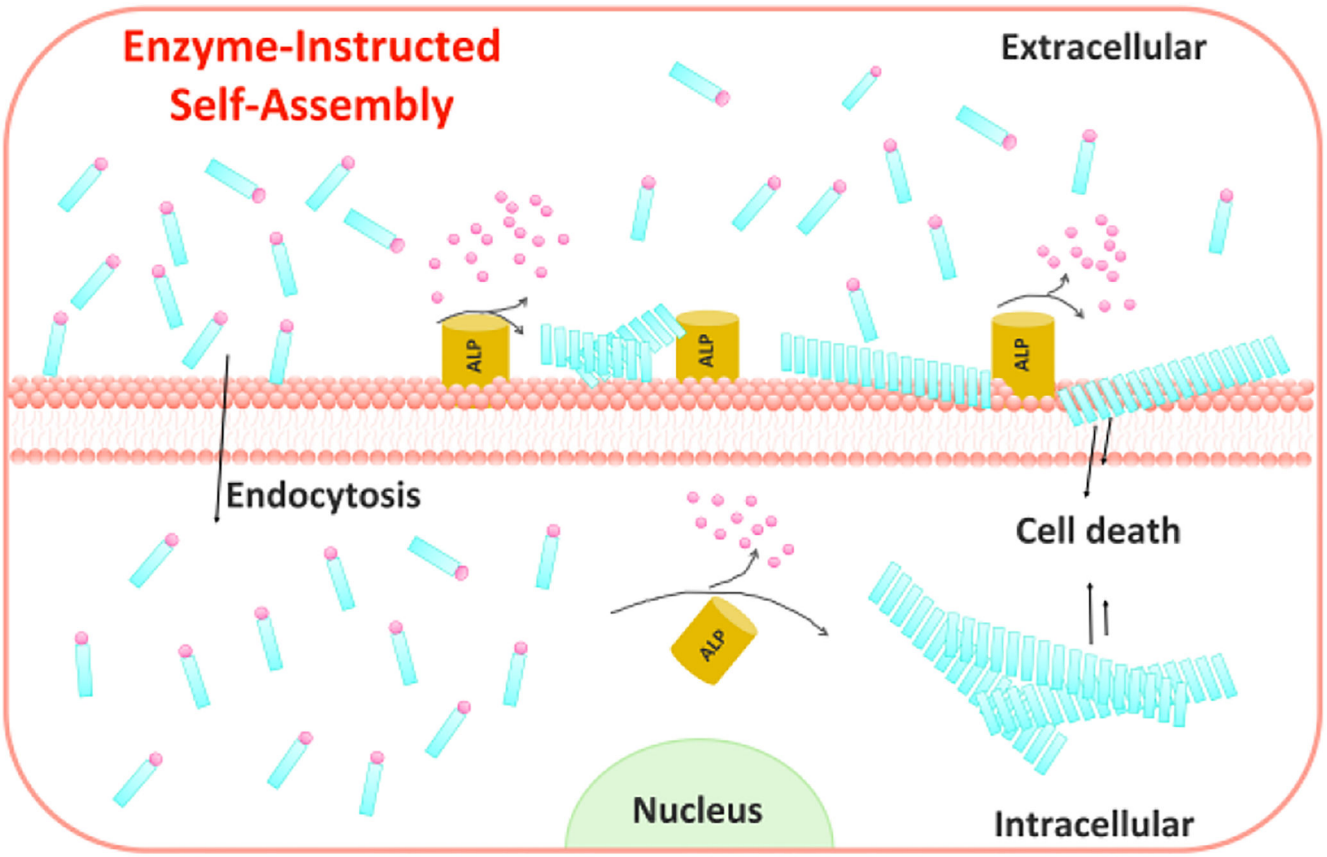

Scheme 1.
The illustration of ALP-instructed self-assembly for inhibiting ovarian cancer cells.

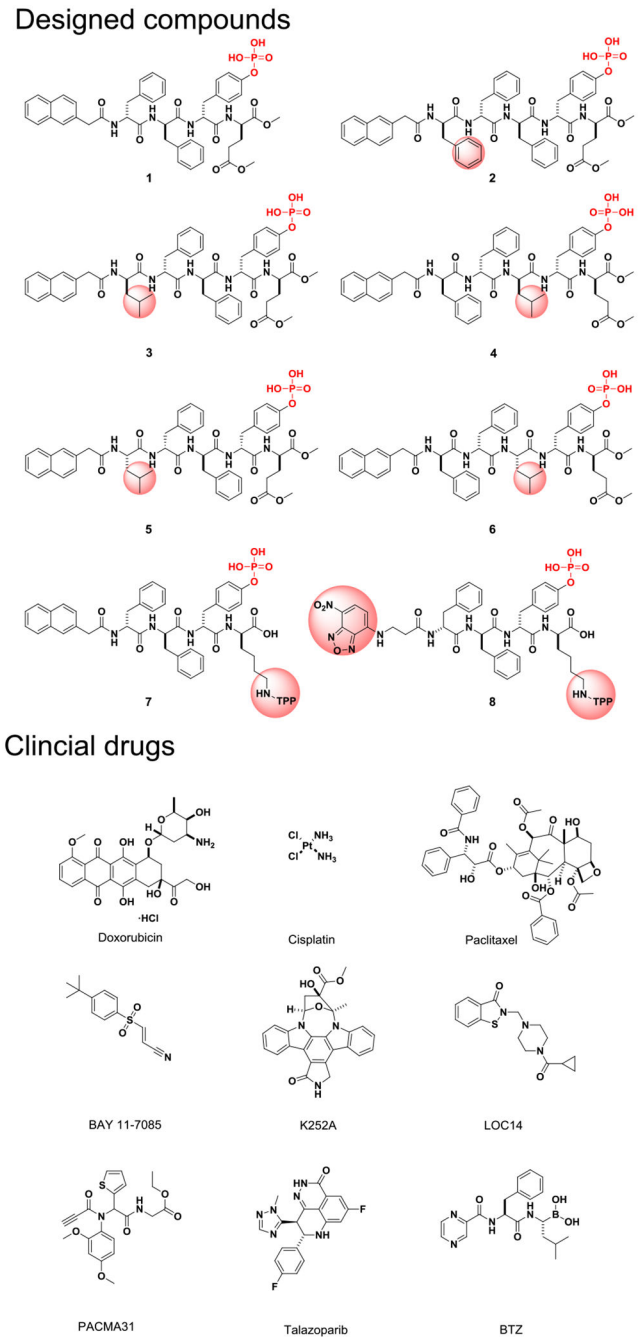

Scheme 2.

The molecular structures of the parent EISA substrate **1** and its analogs **2**-**8** and the structure of the clinical drugs used for combination with **1**.